types, but as these are generally abrupt, we have omitted them here, For example, the Mead transition between types (1) and (2) is described in S. Kurtin, T. C. McGill, and C. Mead, Phys. Rev. Lett. 22, 1433 (1969). In J. C. Phillips, Solid State Commun. 12, 861 (1973), it is shown that the type-(1) → type-(2) transition is determined by the critical polarizability ϵ_c of the nonmetal which separates semiconductors from insulators. This critical polarizability ϵ_c is about 6–7, and the value of ϵ_c is also derived microscopically by Phillips. As noted in Kurtin, McGill, and Mead, the abruptness of the transition suggests a phase transformation, which is the basis of our classification.

[2]Kurtin, McGill, and Mead, Ref. 1.

[3]Phillips, Ref. 1.

[4]W. Schottky, Z. Phys. 118, 539 (1942).

[5]J. Bardeen, Phys. Rev. 71, 717 (1947).

[6]M. J. Turner and E. H. Rhoderick, Solid State Electron. 11, 291 (1968).

[7]M. P. Lepselter and J. M. Andrews, in *Ohmic Contacts to Semiconductors,* edited by B. Schwartz (Electrochemical Society, Princeton, N. J., 1969), p. 159.

[8]J. M. Andrews and M. P. Lepselter, Solid State Electron. 13, 1011 (1970).

[9]J. M. Andrews and F. B. Koch, Solid State Electron. 14, 901 (1971).

[10]C. J. Kircher, Solid State Electron. 14, 507 (1971).

[11]The references for the data on ΔH_f and φ_B are collected in J. C. Phillips and J. M. Andrews, to be published.

[12]Phillips and Andrews, Ref. 11.

[13]L. Pauling, *Nature of the Chemical Bond and the Structure of Molecules and Crystals: An Introduction to Modern Structural Chemistry* (Cornell Univ. Press, Ithica, N.Y., 1960), p. 91 ff.

[14]J. C. Phillips, J. Phys. Chem. Solids 34, 1051 (1973).

[15]The chain structure of tm-metalloid compounds is discussed for the simplest cases (NiAs and MnP structures, to which the simplest silicides belong) by P. Esslinger and K. Schubert, Z. Metallkd. 48, 126 (1957). See especially p. 130.

[16]G. W. Gobeli and F. G. Allen, Phys. Rev. 137, A245 (1965).

[17]A. K. Sinha *et al.*, J. Appl. Phys. 43, 3637 (1972).

[18]L. F. Cordes, M. Garfinkel, and E. A. Taft, NASA Contract Report No. 3-16749, 1974 (unpublished).

[19]J. M. Poate and T. C. Tisone, Appl. Phys. Lett. 24, 391 (1974).

Experimental Contribution to the Summation Problem of Pinning Forces in Type-II Superconductors

G. Antesberger and H. Ullmaier
Institut für Festkörperforschung der Kernforschungsanlage, D 517 Jülich, Germany
(Received 14 April 1975)

The pinning-force density P_v in Nb single crystals containing platelike Nb_2N precipitates shows a strong dependence on the orientation of the precipitates with respect to the flux-line direction. Using purely geometrical arguments this anisotropy can be quantitatively explained by assuming that $P_v \propto K_0^2$, where K_0 is the individual flux-line–defect interaction force. This points to a summation process which is governed by the elastic behavior of the flux lattice.

In an ideal type-II superconductor the flux-line assembly in the mixed state will begin to move and to dissipate energy whenever a force acts on it. Since a transport current perpendicular to the field direction produces such a force, ideal type-II superconductors are not able to carry transport currents without losses. Technologically useful materials therefore contain extended lattice defects (pinning centers) which prevent the flux lattice from moving until the applied force density P_D exceeds a critical value. The corresponding critical current density j_c is given by the condition that P_D just equals the maximum pinning-force density P_v ("critical state"[1,2])

$$-\vec{P}_D = \vec{B} \times \vec{j}_c = \vec{P}_v. \qquad (1)$$

The pinning-force density is a function of the flux density B, the temperature T, and the defect structure of the superconductor. Several measuring techniques have been developed which permit an accurate determination of P_v and reliable data for a vast number of different superconductors and defect structures are now available. However, it is still a point of controversy how these macroscopic results should be correlated with theoretical treatments of the different "microscopic" pinning processes,[3] i.e., with the individual flux-line–defect interaction forces K. Two different views are advocated:

(A) In this approach one assumes that the strong coupling of flux lines to each other prevents them from adjusting to the array of pinning centers in an optimum way. The derivation of P_v from K then involves a complicated summation process which is governed by the elastic behavior of the flux lattice. Theoretical considerations[4-7] show that for a dilute array of pinning centers,

$$P_v = N_v L(k_0 L_z)^2 f(B, C_{ij}(B)), \tag{2}$$

where N_v is the density of pinning centers, L is their linear dimension perpendicular to the driving force, k_0 is the maximum interaction force per unit length, and L_z is the length in the $\vec{B}$ direction over which a pinning center interacts with the flux lines. f is a function of the flux density and a combination of the elastic constants C_{ij} of the flux lattice which depends on the type of the interaction force (point, line, or area force).

(B) In this approach one assumes that in most cases the pinning forces are so strong that they completely disrupt the flux-lattice structure and that its elastic properties can be neglected.[8] Each pinning center then counteracts the driving force with its maximum interaction force and the pinning-force density is given by

$$P_v = N_v (L/a)(k_0 L_z), \tag{3}$$

where $a = (\varphi_0/B)^{1/2}$ is the mean distance between flux lines.

Since the dependence of P_v on B and T is different in Eqs. (2) and (3), a decision in favor of one of the two views should in principle be possible from macroscopic measurements. In practice, however, a quantitative evaluation of such results is often rendered difficult by uncertainties in the theoretical estimates for $K_0 = k_0 L_z$ and in the choice of $f(B, C_{ij})$. The majority of results for metallurgically well-defined samples seems to agree better with Eq. (2) than with Eq. (3) but the conclusions are seldom irrefutable.

An experiment which permits a decision between (A) and (B) from the ratio of P_v values themselves is therefore desirable. A system which fullfills this requirement consists of Nb single crystals of different orientation containing normal-conducting platelike Nb_2N precipitates[9] as pinning centers. They are produced by loading the specimens with 0.3-at.% nitrogen and then aging them for 30 h at 500°C. Electron microscopy shows that the resulting precipitates have a diameter $d \simeq 5000$ Å and a thickness $t \simeq 550$ Å and lie on the $\{100\}$ planes of the bcc Nb lattice. Two cylindrical single-crystal specimens were prepared, one withits axis parallel to the $\langle 100\rangle$ direction and the other parallel to the $\langle 111\rangle$ direction. Since the loading and aging treatments were done simultaneously in the same ultrahigh-vacuum apparatus for both specimens they are metallurgically identical except for the different orientation of the precipitates with respect to the cylinder axes. The applied magnetic field and hence $\vec{B}$ were parallel to the cylinder axis [see Fig. 1(a)]. We may therefore assume that N_v, k_0, $f(B, C_{ij})$, and a are the same for both samples and that differences in the P_v values of the two samples should be caused solely by the different precipitate orientations.

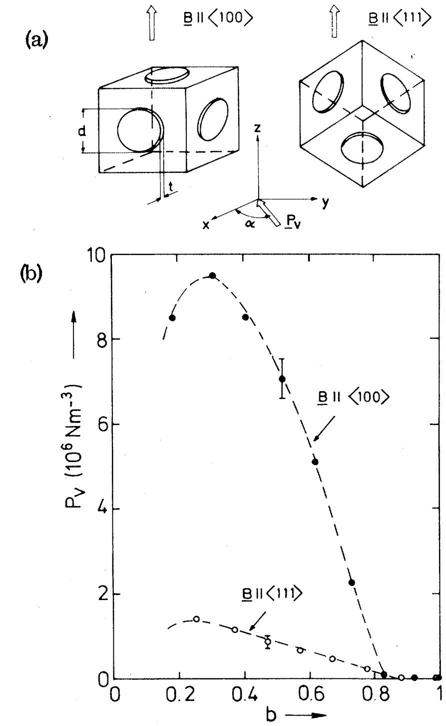

FIG. 1. (a) Orientation of Nb_2N precipitates of diameter d and thickness t with respect to the flux-line direction in Nb crystals with their axes parallel to $\langle 100\rangle$ or $\langle 111\rangle$, respectively. (b) Pinning-force density P_v versus reduced flux density $b = B/B_{c2}$ at 4.2 K. Measurements at different temperatures yield $P_v(b)$ curves of similar shape and confirm that the ratio $P_{v\,100}/P_{v\,111}$ does not depend on B and T.

In other words, N_v and the uncertain quantities k_0 and $f(B, C_{ij})$ cancel out in the ratio $P_{v\,100}/P_{v\,111}$ which depends now only on geometrical parameters of the precipitates and is given by

$$\frac{P_{v\,100}}{P_{v\,111}} = \frac{2\langle L_{100}\rangle \cdot \langle L_{z100}{}^2\rangle + dt^2}{3\langle L_{111}\rangle L_{z111}{}^2} \tag{2a}$$

for case (A), and

$$\frac{P_{v100}}{P_{v111}} = \frac{2\langle L_{100}\rangle \cdot \langle L_{z100}\rangle + dt}{3\langle L_{111}\rangle L_{z111}} \tag{3a}$$

for case (B). In the $\langle 100\rangle$ orientation, $\frac{2}{3}$ of the precipitates have their large dimension $\boldsymbol{d}$ parallel to the flux lines whereas $\frac{1}{3}$ of the plates are perpendicular to $\vec{B}$. In the $\langle 111\rangle$ orientation all three possible orientations are equivalent and act with the same $L_{z111} = t/\sin 35° = 3^{1/2}t$. Since the driving force in a cylindrical sample acts from all angles α in the x-y plane perpendicular to $\vec{B}$ [see Fig. 1(a)], the appropriate averages of the other L and L_z values must appear in Eqs. (2a) and (3a). For thin plates ($t \ll d$) these mean values follow:

$$\langle L_{100}\rangle = 2\pi^{-1}\int_0^{\pi/2} d\cos\alpha\, d\alpha = 2d/\pi, \tag{4}$$

$$\langle L_{111}\rangle \simeq \tfrac{1}{2}(d + d\sin 35°) \simeq 0.8d \tag{5}$$

(actually $\langle L_{111}\rangle$ is given by a complicated integral involving the chords of an ellipse. A numerical evaluation of this integral yields $\langle L_{111}\rangle = 0.87d$),

$$\langle L_{z100}\rangle = \frac{2}{(d/2)\cos\alpha}\int_0^{(d/2)\cos\alpha}\left(\frac{d}{2}\right)\left(1 - \frac{\xi^2}{(d/2)^2\cos^2\alpha}\right)^{1/2} d\xi = \frac{\pi d}{4}, \tag{6}$$

$$\langle L_{z100}{}^2\rangle = \frac{4}{(d/2)\cos\alpha}\int_0^{(d/2)\cos\alpha}\left(\frac{d}{2}\right)^2\left(1 - \frac{\xi^2}{(d/2)^2\cos^2\alpha}\right) d\xi = \frac{2d^2}{3}. \tag{7}$$

Inserting these results into Eqs. (2a) and (3a) yields the relations

$$\frac{P_{v100}}{P_{v111}} = 0.12(d/t)^2 + 0.14 \tag{2b}$$

for case (A), and

$$\frac{P_{v100}}{P_{v111}} = 0.24(d/t + 1) \tag{3b}$$

for case (B); these relations are shown as solid lines in Fig. 2.

Experimentally, the values P_{v100}/P_{v111} and d/t were determined in the following way: The ratio d/t is obtained directly from the electron micrographs and was found to be 9 ± 1.5. The pinning-force densities as a function of B and T were determined by an ac technique described by Ullmaier.[10] In this method a small triangular ripple field is imposed on the large dc field H which determines B. The resulting flux changes are directly related to the critical-flux-density gradient dB/dr and are measured by observing the voltage induced in a pickup coil and around the cylindrical specimens (5 mm diam). An analysis of this voltage yields $P_v = B(dB/dr)(dH/dB)$ which is shown in Fig. 1(b) for the two different samples. Measurements at different B and T (1.2 K< T < 4.2 K) show that the ratio $P_{v100}/P_{v111} = 8 \pm 1$ is practically independent of B and T, which supports the assumption for the derivation of Eqs. (2b) and (3b), namely that the differences in the P_v values for the different samples are solely due to the different precipitate orientations.

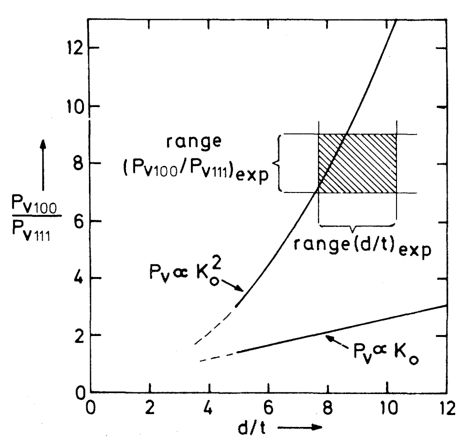

FIG. 2. P_{v100}/P_{v111} as a function of d/t according to Eqs. (2b) and (3b), respectively (solid lines). The hatched rectangle shows the range of the experimentally determined P_{v100}/P_{v111} and d/t values.

In Fig. 2 the range of measured P_{v100}/P_{v111} and d/t values is shown as the hatched rectangle and one can immediately see that there is good agreement between experiment and Eq. (2b). In order to obtain a similar agreement with Eq. (3b) we would have to assume P_{v100}/P_{v111} or d/t values which are definitely far outside the range of experimental uncertainty. This result reinforces the concept (A) that the macroscopic pinning-force density in our system is determined not only by the single-vortex–single-defect interaction K_0 but also by the interaction among vortices themselves which can be taken into account by treating the flux lattice as an elastic medium.

An evaluation of our P_v measurements with Eq. (2) yields K_0 values of several times 10^{-11} N for

$B \to 0$ and $T = 4.2$ K, in agreement with recent neutron diffractions studies[11] in the same material. This indicates that our pinning centers are rather strong compared to other common defects (dilute arrays of single dislocations or grain boundaries, small precipitates, etc.). We therefore expect the above conclusions to apply also for the majority of other dilute systems. However, the results from our model system do not permit predictions about the behavior of very dense $[N_v \gtrsim (10a)^{-3}]$ and/or very strong ($K_0 > 10^{-10}$ N) pinning centers which sometimes occur in materials with technological applications.

We are grateful to Professor J. R. Clem for a critical reading of the manuscript.

[1]C. P. Bean, Phys. Rev. Lett. 8, 250 (1962); H. London, Phys. Lett. 6, 162 (1962).

[2]Y. B. Kim, C. F. Hempstead, and A. R. Strnad, Phys. Rev. Lett. 9, 306 (1962).

[3]For a discussion of possible pinning mechanisms see, e.g., A. M. Campbell and J. E. Evetts, Advan. Phys. 21, 199 (1972); or H. Ullmaier, in *Springer Tracts in Modern Physics* (Springer, Berlin 1975), Vol. 76.

[4]K. Yamafuji and F. Irie, Phys. Lett. A25, 387 (1967).

[5]R. Labusch, Cryst. Lattice Defects 1, 1 (1969).

[6]J. A. Good and E. J. Kramer, Phil. Mag. 22, 329 (1970).

[7]A. M. Campbell and J. E. Evetts, Advan. Phys. 21, 199 (1972).

[8]D. Dew-Hughes, Phil. Mag. 30, 293 (1974).

[9]The metallurgical and superconducting parameters of this system have been investigated in earlier works [G. Antesberger and H. Ullmaier, Phil. Mag. 29, 1101 (1974); T. Schober and G. Antesberger, Scr. Metall. 7, 731 (1973)].

[10]H. Ullmaier, Phys. Status Solidi 17, 631 (1966).

[11]G. Lippmann, in *Proceedings of the International Discussion Meeting on Flux Pinning in Superconductors, St. Andreasberg, Germany, 1974,* edited by P. Haasen (Akademie der Wissenschaften, Göttingen, Germany, 1974).

Tunneling Conductivity in $4Hb$-TaS_2

W. J. Wattamaniuk, J. P. Tidman, and R. F. Frindt
Department of Physics, Simon Fraser University, Burnaby, British Columbia, Canada V5A 1S6
(Received 1 April 1975)

A T^2 behavior for the conductivity across the layers is observed in $4Hb$-TaS_2 crystals below 35 K. This indicates that tunneling occurs between metallic layers separated by an insulating layer. Evidence for thermally activated hopping is observed at higher temperatures.

The superconducting properties of layer compounds intercalated with organic molecules have been explained in terms of superconducting layers coupled via Josephson tunneling.[1] In the normal state in these materials, conduction across the layers should also proceed via tunneling. We present here evidence that quantum mechanical tunneling is the method of conduction across the layers in $4Hb$-TaS_2 at low temperatures and that this material may be a prototype for an intercalated system.

In this Letter we present measurements of electrical conductivity as a function of temperature (T) for the layered transition-metal dichalcogenide $4Hb$-TaS_2. The change in electrical conductivity across the layers with temperature is explained quantitatively by a model whereby localized charge carriers tunnel quantum mechanically from layer to layer, the characteristic signature of a tunneling process being a T^2 dependence of the conductivity at low temperatures. At high temperatures, the small activation energy required to surmount the interlayer barriers dictates that charge transport across the layers proceeds via thermally activated hopping from layer to layer.

The structure of $4Hb$-TaS_2 is made up of S-Ta-S molecular layers, stacked $A, B, C, D, \ldots$.[2] In the A and C layers the S atoms surround the Ta in a trigonal-prism coordination; in the B and D layers the S atoms surround the Ta in an octahedral coordination. The trigonal-prism coordination occurs in $2H$-TaS_2, which has metallic conductivity along the layers[3] and the octahedral coordination is found in $1T$-TaS_2, which is semiconducting.[4] It has been suggested that $4Hb$-TaS_2